

A mutant chaperonin with rearranged inter-ring electrostatic contacts and temperature-sensitive dissociation

B Trevor Sewell¹, Robert B Best^{1,4}, Shaoxia Chen^{2,4}, Alan M Roseman^{2,4}, George W Farr³, Arthur L Horwich³ & Helen R Saibil²

The chaperonin GroEL assists protein folding through ATP-dependent, cooperative movements that alternately create folding chambers in its two rings. The substitution E461K at the interface between these two rings causes temperature-sensitive, defective protein folding in *Escherichia coli*. To understand the molecular defect, we have examined the mutant chaperonin by cryo-EM. The normal out-of-register alignment of contacts between subunits of opposing wild-type rings is changed in E461K to an in-register one. This is associated with loss of cooperativity in ATP binding and hydrolysis. Consistent with the loss of negative cooperativity between rings, the cochaperonin GroES binds simultaneously to both E461K rings. These GroES-bound structures were unstable at higher temperature, dissociating into complexes of single E461K rings associated with GroES. Lacking the allosteric signal from the opposite ring, these complexes cannot release their GroES and become trapped, dead-end states.

The chaperonin GroEL is an 800-kDa, homo-oligomeric double-ring assembly that provides ATP-dependent kinetic assistance to protein folding^{1–4}. It binds non-native polypeptide in an open ring via exposed hydrophobic surfaces that are contacted by hydrophobic side chains lining the GroEL central cavity. Then, upon binding of the lid-like cochaperonin ring, GroES, to the same ring as polypeptide (*cis*), the substrate protein is released from the cavity wall into the now-encapsulated and hydrophilic central cavity where productive folding occurs. ATP hydrolysis in the folding-active ring is followed by ATP binding in the opposite (*trans*) ring, which allosterically triggers ejection of the *cis* ligands: GroES, polypeptide and ADP⁵. For any given cycle of the reaction, released polypeptides that have reached native form or a committed state (no longer recognizable by GroEL) proceed to assemble, if required, and carry out their biological functions. Polypeptides that do not reach native form can be rebound by GroEL to further attempt correct folding or, alternatively, can bind to other chaperones or proteases in the same cellular compartment in a kinetic partitioning mechanism.

As indicated, ATP binding and hydrolysis drive the chaperonin reaction cycle. ATP binding occurs in a cooperative manner: there is positive cooperativity within a ring of seven subunits⁶, but negative cooperativity between the rings, such that ATP binds tightly to only one ring at a time⁷. Because GroES associates only with an ATP-bound ring, asymmetric GroEL–GroES complexes are populated, with a

minority of GroES–GroEL–GroES complexes^{7–9}. Notably, as with many other molecular machines, the binding of ATP carries out the major work of this machine: in *cis*, binding of ATP and GroES triggers productive folding, and in *trans*, the binding of ATP sends an allosteric signal that ejects the *cis* ligands. ATP hydrolysis, by contrast, is used to advance the machine forward through its reaction cycle, weakening the affinity of GroEL for GroES on the *cis* ring and ‘priming’ the *trans*-triggered release of GroES. At the same time, ATP hydrolysis in the *cis* ring allosterically adjusts the *trans* ring to accept non-native polypeptide—that is, the *cis*-ATP GroEL–GroES complex lacks affinity for polypeptide, but after *cis* hydrolysis polypeptide is accepted into the open *trans* ring of a *cis*-ADP complex.

Both the negative cooperativity between rings with respect to ATP binding and the allosteric signaling from an ATP-bound *trans* ring that leads to ejection of the *cis* ligands depend on inter-ring contacts for proper signaling¹⁰. An additional long-range signal sent across the ring-ring interface produces the switch of affinity for polypeptide of the *trans* ring that occurs after *cis* ATP hydrolysis. Finally, the simultaneous binding of both ATP and polypeptide to an open *trans* ring has been observed to accelerate the ejection of *cis* ligands⁵. This indicates that not only adenine nucleotide but also non-native polypeptide can send an allosteric signal across the ring-ring interface. All of these critical inter-ring signaling events in GroEL are transmitted through two equatorially projecting portions of each subunit that make contacts

¹Electron Microscope Unit and Department of Chemistry, University of Cape Town, Rondebosch, South Africa. ²Crystallography Department, Birkbeck College, London WC1E 7HX UK. ³Department of Genetics and Howard Hughes Medical Institute, Yale University School of Medicine, New Haven, Connecticut 06510 USA. ⁴Present addresses: Laboratory of Chemical Physics, National Institute of Diabetes and Digestive and Kidney Diseases, National Institutes of Health, Bethesda, Maryland 20892-0520, USA (R.B.B.) and Medical Research Council Laboratory of Molecular Biology, MRC Centre, Cambridge CB2 1QH, UK (S.C. and A.M.R.). Correspondence should be addressed to H.R.S. (h.saibil@mail.cryst.bbk.ac.uk).

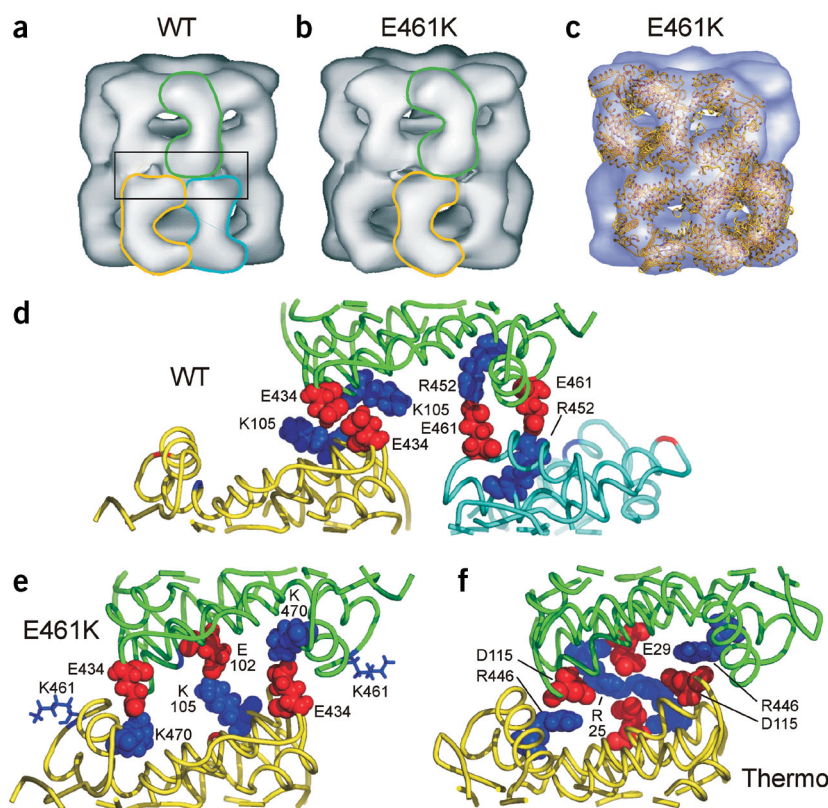


Figure 1 Structural comparison of wild-type (WT) and E461K GroEL. **(a)** Cryo-EM map of wild-type GroEL⁹. Three subunits forming a set of contacts across the ring interface are outlined. **(b)** Equivalent map of GroEL E461K. In this case the inter-ring contacts are between pairs of subunits and two are outlined. **(c)** Docking of wild-type rings that have been rotated to the energy-minimized position shows that there are no large changes in the structure except the rigid-body rotation of one ring relative to the other. **(d–f)** Slabs of the atomic structures centered at the interface, highlighting the residues involved in salt bridge contacts. The boxed area in **a** is enlarged in **d**. **(d)** The inter-ring interface of wild-type GroEL²⁰. The left-hand salt bridge contains Glu434 and Lys105, and the right-hand one contains Arg452 and Glu461. **(e)** The interface of E461K, modeled by energy minimization. An alternative set of salt bridges is predicted, primarily between Glu434 and Lys470 (left and right contacts) and Glu102 and Lys105 (only one pair is formed because of steric hindrance at the central contact). **(f)** The interface between thermosome α subunits (PDB entry 1A6D¹²) for comparison. Panels **c–f** were created with PyMOL (<http://www.pymol.org>).

chaperonin complex and in enabling proper cooperative signaling.

with two adjacent subunits of the opposite ring, with a 1:2 subunit relationship (Fig. 1a,d). The nature of the allosteric transmission through these sites is suggested by cryo-EM analysis of the GroEL–ATP complex¹¹. In that study, ATP binding was shown to distort the ring interface with an overall increase in separation of the rings and tilts of the equatorial domains that change the relative distances of the inter-ring contacts. These distortions are not observed in the crystal lattices of various GroEL–nucleotide complexes.

To understand the structural and mechanistic basis of GroEL cooperativity, which is central to its function in assisting protein folding, we examined a GroEL mutant with defective cooperativity. Here we report a structural analysis of GroEL E461K showing a marked reorganization of the inter-ring interface, causing it to resemble the group II, archaeal and eukaryotic chaperonin structure, in which the interface is formed by a 1:1 subunit interaction¹². *In vitro* studies reveal complete loss of cooperativity of this assembly with respect to ATP binding and hydrolysis. In the presence of ATP and GroES we observed efficient formation of football structures, with GroES bound at either end of the 461 cylinder, reflecting the loss of negative cooperativity. Notably, at elevated temperature these complexes dissociated into complexes of single GroEL rings in complex with GroES, a dead-end state that cannot release its ligands. These observations reveal the importance of proper ring-ring alignment both in maintaining the stability of the

Figure 2 Calculation of the energy of the ring interface in wild-type and mutant GroEL as a function of angle of rotation relative to the position found in wild-type GroEL. The plot covers the asymmetric unit, one-seventh of a complete turn, shown from -26° to $+26^\circ$ of rotation. The energy minimum for the wild-type protein is close to 0° , corresponding to the ring location in wild-type GroEL. For the E461K mutant it is at 16° , corresponding to the rings being in register, consistent with the structure in **Figure 1b**.

RESULTS

An *in vivo* genetic screen had isolated a temperature-sensitive point mutant of GroEL, in which Glu461 in the equatorial interface region was altered to lysine¹³. The E461K mutation alters an electrostatic contact formed with Arg452 to a repulsion and was associated *in vivo* with reduced stability of the assembly, observed as ‘smearing’ of the GroEL-immunoreactive pattern on western blots of native gels, and with temperature-sensitive behavior in several protein folding assays. Defects observed in subsequent *in vitro* studies in polypeptide release were notable in view of the remote position of residue 461 from the apical binding sites some 50–100 Å from the ring interface¹⁴.

To study the structure of the mutant complex, we overexpressed it in *E. coli*, purified it, and examined it by cryo-EM and image reconstruction. We also examined its activities *in vitro* in ATP turnover and protein folding. In addition, the proportions of different assemblies

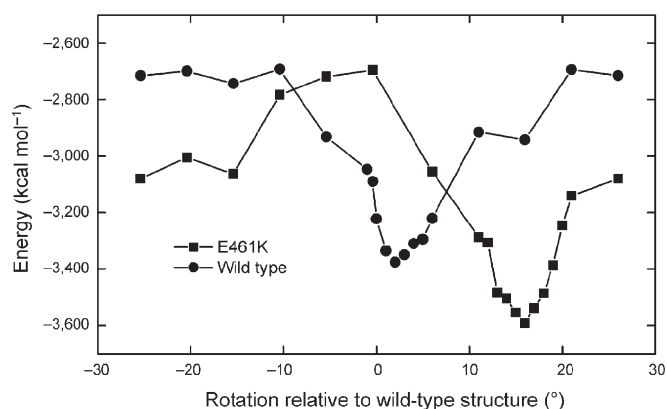
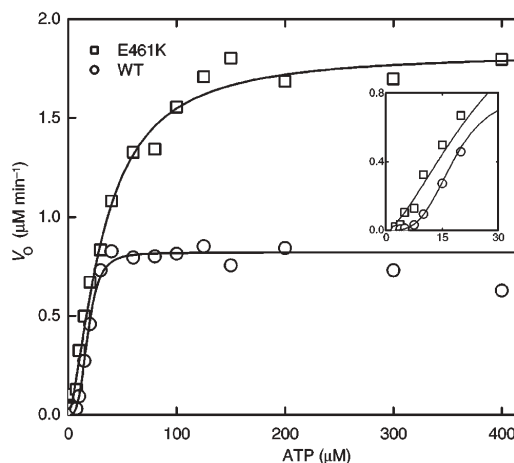


Figure 3 Initial rate of ATPase activity as a function of ATP concentration. The sigmoidal shape of the curve for wild-type (WT) GroEL (inset) results from positive cooperativity of ATP binding, and the reduced ATPase at higher concentrations reflects the negative cooperativity between the GroEL rings. Both these effects are absent in the mutant. The continuous curves were obtained by fitting the data to the Hill equation. In the case of the wild type, the fit is an approximation that does not take into account the effect of negative cooperativity on the shape of the curve at higher ATP concentrations. At the KCl concentration used (5 mM), this effect is small.



formed with GroES at permissive and heat shock temperatures were assessed by negative-stain EM.

GroEL E461K has a rearranged inter-ring interface

The cryo-EM structure of GroEL E461K at a resolution of 24.5 Å clearly reveals the main structural consequence of this mutation. Although the maps of wild-type and E461K GroEL are superficially similar (Fig. 1a,b), examination of the relationship between the rings reveals a complete reorganization of the ring interface in the mutant. The opposing subunits of E461K rings are in register, and the contacts are 1:1 instead of 1:2 (Fig. 1b). At this resolution the maps appear identical except for an 18° rigid body rotation about the seven-fold symmetry axis of one ring relative to the other in the

mutant (Fig. 1c). The contact regions between rings are enlarged and shown as atomic structures in Fig. 1d–f. The E461K interface (Fig. 1e) is derived from an energy-minimized model (see below), and the group II thermosome interface is shown for comparison (Fig. 1f).

Computation of the energy as a function of the angle of rotation about the seven-fold symmetry axis for wild-type and mutant GroEL gives results that are consistent with the EM reconstructions (Fig. 2). There is an energy minimum close to 0° for wild-type GroEL, corresponding to the offset ring conformation of the normal structure (Fig. 1a,d). For E461K, a minimum is seen at 16°, corresponding to the in-register alignment seen in the mutant structure (Fig. 1b,c). The electrostatic contributions to the overall energy were dominant. The energy-minimized model of the E461K interface enables identification of ion pair residues likely to interact in the mutant (Fig. 1e). The model predicts that Lys470 and Glu102, residues near the interface but not involved in any contacts in the wild-type structure, are recruited to form contacts, and that the mutant Lys461 side chain rotates away from the contact region. The predicted salt bridges are formed primarily between Glu434 and Lys470, and between Glu102 and Lys105. Other residues, including Asp435, Arg445 and Arg452, are close enough to make a substantial contribution to the interaction.

Defective activity *in vitro*

ATPase activity is increased in the E461K mutant relative to wild-type GroEL across a range of ATP concentrations (Fig. 3), reflecting the loss of negative cooperativity. The nonsigmoidal shape of the ATPase curve at low ATP concentration (Fig. 3, inset) indicates that positive cooperativity is also lost in the mutant. Chaperonin function was tested by assaying the refolding of denatured mitochondrial MDH. At 25 °C, the mutant chaperonin supported MDH refolding, but this was defective

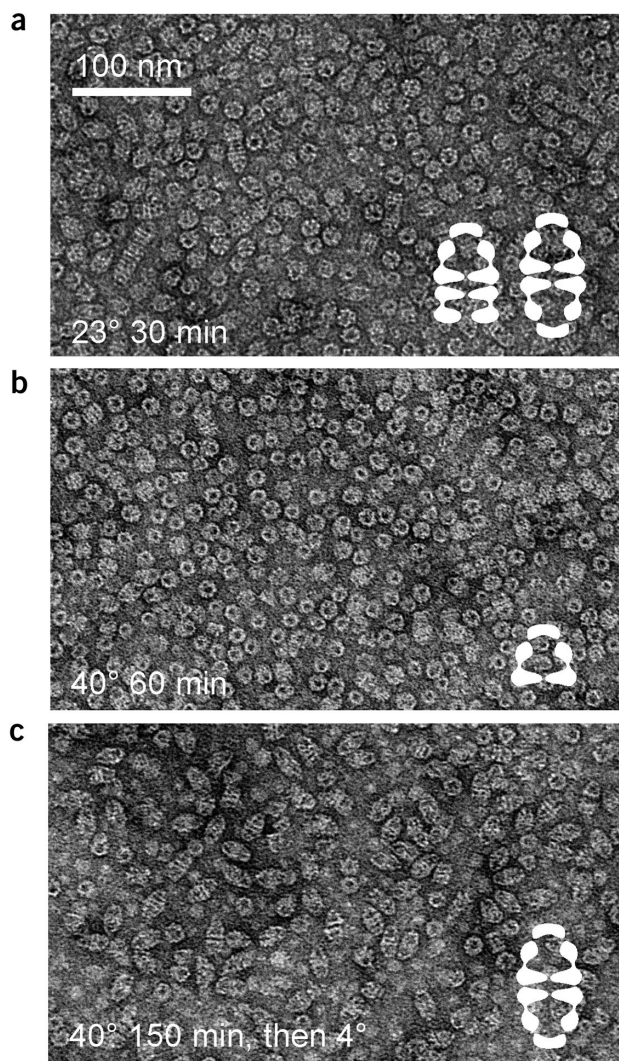


Figure 4 Temperature sensitivity of GroEL E461K-GroES complexes in the presence of 4 mM ATP observed by negative-stain EM. (a) Complexes incubated at 23 °C. (b) Complexes incubated at 40 °C. (c) Complexes incubated at 40 °C, then cooled down to 4 °C. The cartoon symbols indicate the predominant complexes present in each sample. In a, side views of GroEL, GroEL-GroES (bullet-shaped complexes) and GroES-GroEL-GroES (football-shaped complexes) are visible, as well as end views. The complexes in b are mostly end views. These are attributed to football complexes that have split into single GroEL rings, each with a bound GroES (see text). Upon cooling (c), the split complexes reassociate and mainly football complexes are seen.

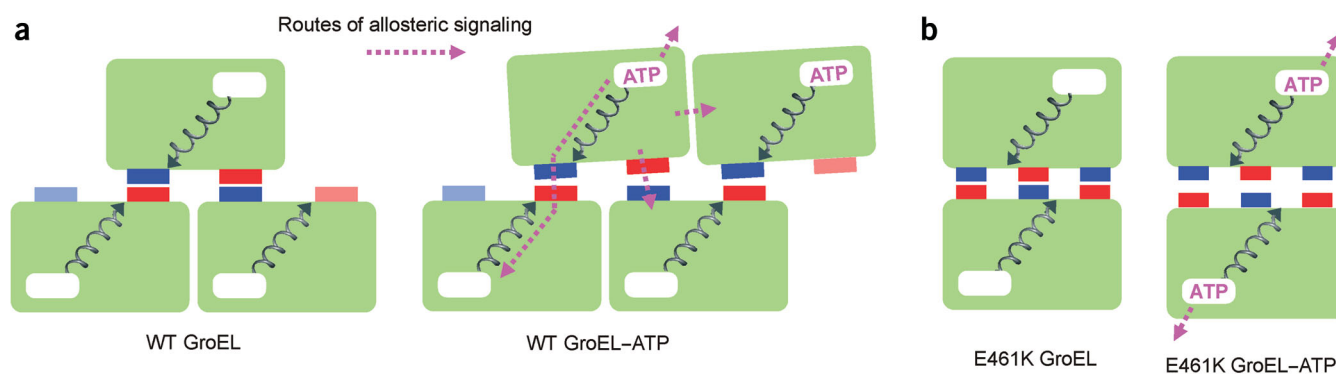


Figure 5 Allosteric communication in wild-type (WT) and E461K GroEL. **(a)** Schematic diagram of three equatorial domains (green) at the front of the GroEL complex, showing the staggered contacts (red and blue boxes) made across the ring interface. Helix D (residues 87–109) is shown as a coil. The view is as in **Figure 1d**. On the right, the domain tilting accompanying ATP binding in one ring¹¹ is represented. An additional domain in the upper ring is included to show the conformational strain between adjacent equatorial domains within the ATP-bound ring, as indicated by purple dashed arrows. Both the intra- and inter-ring interfaces between adjacent equatorial domains are distorted by the domain tilting. The arrow extending from the ATP-binding pocket represents the propagation of conformational changes to the intermediate and apical domains. **(b)** The situation in GroEL E461K is simpler, with the equatorial domains in an eclipsed conformation at the interface. Three salt-bridge contacts are predicted by the simulation (**Figs. 1e** and **2**). Helix D connects to the central contact. Owing to the lack of negative cooperativity, ATP fills both rings simultaneously. The ring interface weakens, but changes communicated to the central contact are unlikely to lead to domain tilting.

at 37 °C, with no recovery of MDH activity at 1 mM ATP, and ~50% recovery at 10 mM ATP (data not shown). Similar results have been obtained previously¹⁵, although the loss of positive cooperativity was not resolved in that study.

Structural effects of ATP and elevated temperature

Incubation at temperatures up to 60 °C does not cause any changes in the structures of isolated wild-type or E461K GroEL observable by negative-stain EM (data not shown). However, substantial effects were observed when we compared the proportions of different assemblies in preparations of wild-type and E461K GroEL incubated with GroES and ATP, at 23 and 40 °C. The loss of negative cooperativity in E461K is reflected in the higher proportion of double-sided, GroES–GroEL–GroES ‘football’ complexes of the mutant protein (**Fig. 4a**) than in the corresponding wild-type preparation. For the mutant at 40 °C, the football views gradually disappear with increasing incubation time, and are replaced by relatively featureless rings, many lacking the characteristic seven-fold symmetry of GroEL end views, and also by triangular views (**Fig. 4b**). The footballs rapidly reappear upon cooling (**Fig. 4c**). These findings were verified by counting large data sets in a systematic time course experiment on wild-type and E461K complexes incubated at 23 and 40 °C, and then cooled to 4 °C. The counts show that the proportion of football plus bullet side views is in the range expected for wild type (data not shown) at 40 °C (30%), low in E461K at 23 °C (4%) and very low in E461K at 40 °C (1.5%), but that it increases markedly upon cooling of the E461K samples to 4 °C (15%). The heated mutant sample contains a great majority of end views (**Fig. 4b**).

The featureless rings and triangular views can be identified as complexes of GroES with a single ring of GroEL. These ‘half-footballs’ are fairly round particles, which adopt a more uniform distribution of orientations on the EM grid than the cylindrical complexes containing double-ring GroEL. The triangles can be recognized as side views of the *cis* cavity of GroEL–GroES complexes, or half-footballs. Although images of double-ring complexes in the presence of ATP or of ATP and GroES were scarce, we obtained cryo-EM reconstructions of these complexes. Consistent with a disordered interface between the two rings, these maps were of poor quality, with rotationally smeared features (data not shown).

DISCUSSION

In this study we have described a GroEL chaperonin mutant in which the normal inter-ring electrostatic contacts have been replaced, as the result of mutation of a charge attraction to one of repulsion, with a new set of electrostatic contacts that position the two rings 18° out of normal register. The price paid for such a rearrangement is complete loss of cooperativity with respect to ATP binding and hydrolysis. Both the negative cooperativity between rings and also the positive cooperativity within them are abolished, supporting the idea that the lines of cooperative communication between rings are inextricably linked to communication between subunits within the rings¹⁶. Despite the complete loss of cooperativity with respect to ATP, this assembly remains partly functional in protein folding, observed both *in vivo* during the earlier study of the temperature-sensitive mutant¹³ and here and elsewhere¹⁵ *in vitro*. That is, there is sufficient residual allosteric function to allow productive cycles of binding and release of substrate polypeptide. How does the temperature sensitivity come about?

Considering the formation of the folding chamber, we know from studies of single-ring GroEL (SR1) that binding of non-native substrate, followed by ATP- and GroES-induced conformational change, can lead to the normal folding of substrate inside the cavity associated with one round of ATP hydrolysis^{5,17}. The result of these steps is a stable, dead-end complex, SR1–ADP–GroES, with the folded substrate trapped inside the cavity. It seems likely that the steps resulting in formation of the GroEL–GroES chamber occur fairly normally in GroEL E461K. However, owing to the loss of negative cooperativity with respect to ATP, GroES binds simultaneously to both rings of the E461K assembly, so that football complexes predominate. The football conformation is likely to place extra strain on the equatorial domains¹⁸.

The problem in E461K arises in the next phase of the functional cycle. In wild-type complexes, ATP hydrolysis in the GroES-bound *cis* ring weakens the binding of GroES but does not result in its release⁵. Subsequently, ATP binding to the *trans* ring triggers the release of GroES, allowing the escape of folded substrate and trapped ADP. This communication from *trans* to *cis* rings must occur through conformational changes in the ring interface. In wild-type complexes, ATP binding weakens the ring interface and distorts it by tilting the equatorial domains (ref. 11; N.A. Ranson (Biochemistry and Microbiology

Department, Leeds University), D.K. Clare (Crystallography Department, Birkbeck College), G.W.F., A.L.H. and H.R.S., unpublished data). In E461K complexes, however, the ring interface is less able to support the distorted and weakened interactions of nucleotide-bound states, and thus the ATP- and GroES-bound complexes are much less stable than in the case of the wild-type protein. Indeed, at elevated temperature, the football complexes fall apart into single-ring GroEL–GroES complexes (Fig. 3b). Without the apposed equatorial domains of an opposite ring to provide the trigger, GroES release from these single-ring complexes is greatly impaired, as in the designed SR1 complex. The dissociation of the interface is reversed upon cooling, with the rapid reappearance of footballs (Fig. 3c). Notably, this marginally stable, wrongly arranged inter-ring interface can support some degree of normal cycling at reduced temperature.

Insight into the ability of the mutant to retain some normal GroEL function despite the complete rearrangement of the ring interface contacts and its instability comes from an unexpected parallel with a different subfamily of chaperonins. Notably, the 1:1 arrangement of subunits across the interface has a natural precedent. An interface with in-register subunit contacts occurs in the group II chaperonins, such as the archaeal thermosome¹². Because the group II chaperonins also exhibit negative cooperativity¹⁹, it must be transmitted across the ring interface by different interactions than the ones in E461K. The mutant interface bears a marked resemblance to that of the thermosome (Fig. 1f), except that the inter-ring separation in the group II structure is smaller, and the interaction seems tighter. Perhaps the stronger interface enables this chaperonin subfamily to withstand nucleotide-induced distortions of the equatorial contacts in the 1:1 geometry without excessive weakening of the contacts.

These findings provide new insights into the mechanism of negative cooperativity in chaperonins. From our earlier work on GroEL–ATP complexes¹¹, we know that the equatorial domains tilt upon ATP binding, and that the interface between the rings is distorted. The ATP-binding site is linked through helix D (residues 87–109) to the left inter-ring contact (Figs. 1d and 5a). In the E461K mutant, helix D does not connect to an inter-ring contact at the side of the domain (Figs. 1e and 5b) and there is no negative cooperativity. This comparison suggests that negative cooperativity depends on equatorial domain tilting and interface distortion transmitted through helix D to one side of the domain, providing leverage for tilting. We predict that the equatorial domains in group II chaperonins will also tilt when ATP is bound in one ring, because the ATP binding site is directly linked to the left and right contacts (Fig. 1f).

The positive and negative cooperativity mechanisms are clearly interrelated in the central role of the nucleotide-binding, equatorial domains, which form the major intra-ring contacts and all the inter-ring contacts²⁰. By virtue of its unanticipated effects on the assembly of the complex, the E461K mutation has provided us with a novel and informative probe of the levers operating the intricate allosteric mechanism of chaperonins.

METHODS

Protein purification and activity assays. E461KGroEL E461K was overexpressed and purified as described¹⁹. The buffer for EM contained 20 mM Tris, 5 mM KCl, 10 mM MgCl₂, pH 7.4. ATPase activity was measured as described²¹. Refolding of MDH was carried out as described²².

Cryo-EM. Specimens containing 1 μM GroEL E461K were flash-frozen in liquid ethane and imaged at –170 °C on a JEOL 2010 electron microscope at 200 kV using an Oxford Instruments CT3500 cryostage. The images were recorded with an electron dose of 10 e[–] Å^{–2} and with a defocus range of 1–2 μm at 30,000× on Kodak SO163 film. Images were digitized on a Leafscan 45 linear

CCD scanner (Ilford) with a step size of 20 μm, which corresponds to a pixel size of 6.67 Å on the specimen. Particle selection was done with the MRC program Ximdisp²³. Three-dimensional reconstruction from a data set of 1,500 particle images was done by projection matching with SPIDER²⁴, using the EM structure of wild-type GroEL as a starting model⁹. The resolution was measured by Fourier shell correlation, using the 0.5 correlation criterion.

Negative-stain EM. A Heraeus oven was modified to allow the preparation of negative-stain grids at a known fixed temperature. The door of the oven was replaced with a perspex front with two 15-cm circular holes to allow hand access. A thermostatic oven controller (RS Components) and fan were added. In addition to the controller, temperature was monitored by a thermocouple in the immediate vicinity of the sample and a mercury thermometer at the top of the oven. The temperature of the chamber was 40 ± 2 °C during the experiment. Stain and pipette tips were allowed 5 min to reach the set temperature. Grids were prepared in the oven by depositing a 3-ml droplet onto the grid and then rinsing with 3% w/v uranyl acetate. Images were recorded at 42,000× and 100 kV on a Tecnai T10 electron microscope. Images were collected from two repeats of a time course experiment over 2.5 h, comparing complexes formed with wild-type or E461K GroEL (0.1 μM), GroES (>0.2 μM) and ATP (4 mM). A total of 2,000–5,000 particles were counted, independently by two observers, from each micrograph.

Energy calculations. A coordinate set for E461K was generated by substituting a lysine side chain for Glu461 in the GroEL structure (PDB entry 1OEL)²⁵. Hydrogen atoms were added using the HBUILD facility of CHARMM²⁶, and all energy calculations were done with CHARMM²⁷ using the CHARMM 22 force-field²⁸, with a distance-dependent dielectric to approximate the effect of solvent. The coordinate model was generated from a pair of subunits, one from each ring, the interactions with the remaining subunits being inferred from C7 symmetry. For each angular displacement from the native orientation, an energy minimization was done as follows: atoms >8 Å from the equatorial plane were ‘fixed,’ but allowed to interact with the remainder of the system. The energy was then minimized by 40 steps of steepest descent and 1,000 steps of conjugate gradient minimization, after which the energies and coordinates were written out. Changing to a constant dielectric of 1 or 4 did not qualitatively alter the shape of the energy profiles.

Coordinates. The EM density map of GroEL E461K has been deposited in the EM database (accession code EMD-1095).

ACKNOWLEDGMENTS

We thank R. Westlake, D. Houldershaw and S. Terrill for computing support, W. Fenton and M. Karplus for advice and discussion, M. Jaffer and W. Williams for help with particle counting, and The Wellcome Trust and the Howard Hughes Medical Institute for financial support.

COMPETING INTERESTS STATEMENT

The authors declare that they have no competing financial interests.

Received 1 June; accepted 15 September 2004

Published online at <http://www.nature.com/nsmb/>

1. Sigler, P.B. *et al.* Structure and function in GroEL-mediated protein folding. *Annu. Rev. Biochem.* **67**, 581–608 (1998).
2. Brinker, A. *et al.* Dual function of protein confinement in chaperonin-assisted protein folding. *Cell* **107**, 223–233 (2001).
3. Saibil, H.R. & Ranson, N.A. The chaperonin folding machine. *Trends Biochem. Sci.* **27**, 627–632 (2002).
4. Todd, M.J., Lorimer, G.H. & Thirumalai, D. Chaperonin-facilitated protein folding: optimization of rate and yield by an iterative annealing mechanism. *Proc. Natl. Acad. Sci. USA* **93**, 4030–4035 (1996).
5. Rye, H.S. *et al.* GroEL–GroES cycling: ATP and nonnative polypeptide direct alternation of folding-active rings. *Cell* **97**, 325–338 (1999).
6. Gray, T.E. & Fersht, A.R. Cooperativity in ATP hydrolysis by GroEL is increased by GroES. *FEBS Lett.* **292**, 254–258 (1991).
7. Yifrach, O. & Horowitz, A. Nested cooperativity in the ATPase activity of the oligomeric chaperonin GroEL. *Biochemistry* **34**, 5303–5308 (1995).
8. Burston, S.G., Ranson, N.A. & Clarke, A.R. The origins and consequences of asymmetry in the chaperonin reaction cycle. *J. Mol. Biol.* **249**, 138–152 (1995).
9. Roseman, A.M., Chen, S., White, H., Braig, K. & Saibil, H.R. The chaperonin ATPase cycle: mechanism of allosteric switching and movements of substrate-binding domains in GroEL. *Cell* **87**, 241–251 (1996).

10. Rye, H.S. *et al.* Distinct actions of *cis* and *trans* ATP within the double ring of the chaperonin GroEL. *Nature* **388**, 792–798 (1997).
11. Ranson, N.A. *et al.* ATP-bound states of GroEL captured by cryo-electron microscopy. *Cell* **107**, 869–879 (2001).
12. Ditzel, L. *et al.* Crystal structure of the thermosome, the archaeal chaperonin and homolog of CCT. *Cell* **93**, 125–138 (1998).
13. Horwich, A.L., Low, K.B., Fenton, W.A., Hirshfield, I.N. & Furtak, K. Folding in vivo of bacterial cytoplasmic proteins: role of GroEL. *Cell* **74**, 909–917 (1993).
14. Fenton, W. A., Kashi, Y., Furtak, K. & Horwich, A. L. Residues in chaperonin GroEL required for polypeptide binding and release. *Nature* **371**, 614–661 (1994).
15. Sot, B., Galan, A., Valpuesta, J.M., Bertrand, S. & Muga, A. Salt bridges at the inter-ring interface regulate the thermostat of GroEL. *J. Biol. Chem.* **277**, 34024–34029 (2002).
16. Yifrach, O. & Horovitz, A. Two lines of allosteric communication in the oligomeric chaperonin GroEL are revealed by the single mutation Arg196→Ala. *J. Mol. Biol.* **243**, 397–401 (1994).
17. Weissman, J.S. *et al.* Mechanism of GroEL action: productive release of polypeptide from a sequestered position under GroES. *Cell* **83**, 577–587 (1995).
18. Ma, J., Sigler, P.B., Xu, Z. & Karplus, M. A dynamic model for the allosteric mechanism of GroEL. *J. Mol. Biol.* **302**, 303–313 (2000).
19. Kafri, G. & Horovitz, A. Transient kinetic analysis of ATP-induced allosteric transitions in the eukaryotic chaperonin containing TCP-1. *J. Mol. Biol.* **326**, 981–987 (2003).
20. Braig, K. *et al.* The crystal structure of the bacterial chaperonin GroEL at 2.8 Å. *Nature* **371**, 578–586 (1994).
21. Horovitz, A., Bochkareva, E.S., Kovalenko, O. & Girshovich, A.S. Mutation Ala2→Ser destabilizes intersubunit interactions in the molecular chaperone GroEL. *J. Mol. Biol.* **231**, 58–64 (1993).
22. Ranson, N.A., Dunster, N.J., Burston, S.G. & Clarke, A.R. Chaperonins can catalyse the reversal of early aggregation steps when a protein misfolds. *J. Mol. Biol.* **250**, 581–586 (1995).
23. Crowther, R.A., Henderson, R. & Smith, J.M. MRC image processing programs. *J. Struct. Biol.* **116**, 9–16 (1996).
24. Frank, J. *et al.* SPIDER and WEB: processing and visualization of images in 3D electron microscopy and related fields. *J. Struct. Biol.* **116**, 190–199 (1996).
25. Braig, K., Adams, P. D. & Brunger, A. T. Conformational variability in the refined structure of the chaperonin GroEL at 2.8 Å resolution. *Nat. Struct. Biol.* **2**, 1083–1094 (1995).
26. Brunger, A.T. & Karplus, M. Polar hydrogen positions in proteins—empirical energy placement and neutron diffraction comparison. *Proteins* **4**, 148–156 (1988).
27. Brooks B.R. *et al.* CHARMM: a program for macromolecular energy, minimization, and dynamics calculations. *J. Comp. Chem.* **4**, 187–217 (1983).
28. MacKerell, A.D. Jr. *et al.* All-atom empirical potential for molecular modeling and dynamics studies of proteins. *J. Phys. Chem. B* **102**, 3586–3616 (1998).